NMO surfaces and Dix-type formulae in heterogeneous anisotropic media

Vladimir Grechka and Ilya Tsvankin
Center for Wave Phenomena

ABSTRACT

The most stable portion of pure-mode reflection moveout recorded on conventional spreads is represented by the normal-moveout (NMO) velocity even in heterogeneous anisotropic media. Grechka and Tsvankin have recently shown that azimuthal variation of the NMO velocity measured at a horizontal plane has an *elliptical* form regardless the type of anisotropy and heterogeneity of the subsurface. Here, we extend their work further relaxing the original constraint that a common-midpoint (CMP) line belongs to a horizontal plane and considering CMP lines arbitrary oriented in 3-D space (e.g, a CMP line may be inside a vertical or an oblique borehole).

We show that the NMO velocity, treated as a function of direction in 3-D space, forms a quadratic surface which is usually either an *ellipsoid*, or an *one sheeted hyperboloid*, or an *elliptical cylinder*. The NMO ellipse examined by Grechka and Tsvankin represents the cross-section of this surface by the horizontal plane. Since any quadratic surface in its canonical form can be written in terms of a 3×3 symmetric matrix, it is generally determined by *six* quantities. We prove, however, that the whole NMO surface can be reconstructed from NMO velocity measurements along at least *three* different directions (or from NMO ellipse), and the remaining quantities are computed in a straightforward way from the Christoffel equation given the local values of elastic stiffness coefficients. If more than three velocity measurements along directions which do not belong to a single plane are available, the equation for the NMO surface allows one to constrain additional medium parameters compared to those constrained by the NMO ellipse.

The NMO surfaces introduced in the paper provide a natural basis for building the Dix-type averaging and differentiation algorithms in *generally heterogeneous* anisotropic media. These algorithms operate with certain cross-sections of the NMO surfaces and do *not* require any components of the slowness vector to be preserved along a ray. As a special case of such algorithms, we derive the Dix-type formulae in a medium that contains several homogeneous anisotropic layers separated by plane *arbitrarily dipping* interfaces. Our Dix-type formulae average or differentiate the cross-sections of NMO surfaces by the medium interfaces. In the case of VTI layers, the presence of dipping intermediate interfaces makes P-wave NMO ellipses measured in a horizontal plane depend on individual values of interval Thomsen's coefficients ϵ and δ, thus, bearing a potential for *depth* processing in VTI media based on P-wave surface reflection data.

Key words: NMO surfaces, Dix-type procedures in heterogeneous media

Introduction

The normal-moveout (NMO) velocity $V_{\rm nmo}$ estimated from reflection traveltimes recorded in common-midpoint (CMP) geometry on conventional spreads provides the most reliable information about velocity and anisotropy of the subsurface. Interpretation of this infor-

mation in terms of medium parameters, however, is not automatic and has to be based on theoretical relations between measured NMO velocities and the parameters of a chosen subsurface model. Such relations become especially complex and estimated parameters nonunique if the chosen model is heterogeneous and anisotropic. Nonetheless, even in this the most general and difficult case, significant simplification comes from the fact that dependence of NMO velocity on the orientation of CMP line, which can be exploited for parameter estimation, has an explicit and simple form. For example, Grechka and Tsvankin (1998a) examined reflection traveltimes of pure modes recorded at a fixed CMP location along lines of different azimuths α in the horizontal plane $x_3 = \text{const}$ and showed that the azimuthal variation of the normal-moveout velocity $V_{\rm nmo}(\alpha)$ is an *ellipse* for arbitrary anisotropy and heterogeneity of the subsurface unless reflection traveltimes decrease with the offset in some directions. The reason for such simplicity and generality is that the NMO velocity expresses the wavefront curvature at the zero-offset and, therefore, its azimuthal variation has to be a quadratic function.

Realizing that $V_{\rm nmo}(\alpha)$ has an elliptical behavior not only allows one to build relatively simple algorithms for azimuthal velocity analysis (e.g., Corrigan et al., 1996; Grechka and Tsvankin, 1999b) but also provides a basis for constructing the Dix-type averaging and differentiation procedures for NMO ellipses in anisotropic vertically inhomogeneous media (Grechka et al., 1999). While the Dix-type averaging can be viewed as an effective method for computing azimuthally varying NMO velocities, the Dix-type stripping is a viable tool for obtaining interval NMO ellipses and, thus, the interval medium parameters. The techniques for parameter estimation using the Dix-type differentiation of NMO ellipses (the so called "the generalized Dix formula") of Grechka et al. (1999) have been developed for the most important anisotropic models in seismic exploration: transversely isotropic media with either vertical, horizontal, or tilted symmetry axis (Contreras et al., 1999; Grechka and Tsvankin, 1998b), and orthorhombic media (Grechka and Tsvankin, 1999a).

Although it may seem that NMO ellipses and related processing techniques fully satisfy the requirements of modern 3-D multi-azimuth acquisition geometries, it is possible to develop the theory of normal moveout further. Such a development is associated with the fact that there is no reason to restrict the theory by considering only the NMO velocities measured in a *horizontal* plane. One can imagine recording reflection arrivals along an oblique or a vertical borehole. In this case, if CMP geometry is employed, the obtained NMO velocity $V_{\rm nmo}$ is going to be a function of direction $\mathcal{L}$ in *3-D space*. Thus, the ends of the vectors $V_{\rm nmo}(\mathcal{L})$ plotted from a common origin are going to form a *surface* in space. Following the logic of Grechka and Tsvankin (1998a), it is straightforward to predict that $V_{\rm nmo}(\mathcal{L})$ is a *quadratic* surface. Here, we derive the surfaces $V_{\rm nmo}(\mathcal{L})$ in arbitrary anisotropic heterogeneous media and prove that $V_{\rm nmo}(\mathcal{L})$ is always an *elliptical cylinder* if medium is homogeneous in the vicinity of CMP location and reflection traveltime does not decrease with the offset. The NMO ellipses $\mathbf{W}$ examined by Grechka and Tsvankin (1998a) become simply cross-sections of more general NMO surfaces by the horizontal plane passing through the coordinate origin.

While the above discussion may seem purely theoretical, it has a certain practical value even though we probably cannot measure $V_{\rm nmo}$ along many different directions $\mathcal{L}$ in space. The immediate consequence of the fact that $V_{\rm nmo}(\mathcal{L})$ is a quadratic surface is that it can be represented by a 3×3 symmetric matrix $\mathbf{U}$ which is determined by six independent quantities U_{km} ($k \le m$, $m = 1, 2, 3$). Thus, *six* is the maximum number of combinations of medium parameters which can be estimated from spatial variation of NMO velocity for a given reflection at a certain CMP location. It is important that the whole surface $\mathbf{U}$ can be reconstructed from its cross-section by an arbitrary plane, for instance, from a given NMO ellipse $\mathbf{W}$. The elements U_{km} which are not determined by the ellipse $\mathbf{W}$ can be found by differentiating the Christoffel equation if elastic stiffness coefficients c_{ij} are known at the CMP location. Since the NMO ellipse by itself can be inverted for the medium parameters (e.g., Contreras et al., 1999; Grechka and Tsvankin, 1998a, 1998b, and 1999a), any velocity measurements *outside* the plane specified by the NMO ellipse can be used to obtain additional parameters. To illustrate this point, we show that P-wave NMO surface measured from a dipping reflector beneath a homogeneous transversely isotropic medium with a vertical symmetry axis (VTI model) allows estimating Thomsen's (1986) anisotropic coefficients ϵ and δ *individually* whereas the NMO ellipse at the horizontal plane constrains only the anellipticity coefficient η (Alkhalifah and Tsvankin, 1995) which approximately equals to the difference $\epsilon - \delta$.

The usefulness of the theory discussed in the paper goes well beyond establishing the maximum number of parameter combinations invertible from NMO velocity measurements and estimating anisotropic coefficients for particular models. The mere appearance of elements U_{km} of the matrix $\mathbf{U}$ describing the NMO surface $V_{\rm nmo}(\mathcal{L})$ allows constructing the Dix-type relations which can be used to trace the whole NMO surface along a ray. Those relations lead to the Dix-type averaging and differenti-

ating algorithms in arbitrary *inhomogeneous* anisotropic media, i.e., in media where *neither one* component of the slowness vector is preserved along the ray. As an example of such algorithms, we construct the Dix-type formulae for a medium that consists of a set of homogeneous anisotropic layers separated by plane *arbitrarily dipping* interfaces. Our formulae operate with cross-sections of the NMO surfaces by the medium interfaces. In the practically important case of VTI layers, the presence of intermediate dipping interfaces causes dependence of P-wave NMO ellipses recorded in a horizontal plane on interval values of vertical velocities and Thomsen's coefficients ϵ and δ, thus, indicating a theoretical possibility of *depth* processing in VTI media based solely on surface P-wave data.

NMO surfaces in inhomogeneous anisotropic media

General formulation

Here, we give an exact formula for pure-mode NMO velocity $V_{\rm nmo}$ recorded along an arbitrary oriented CMP line $\mathcal{L} = [\mathcal{L}_1,\, \mathcal{L}_2,\, \mathcal{L}_3]$ in inhomogeneous anisotropic media. The dependence $V_{\rm nmo}(\mathcal{L})$, derived in Appendix A, is given by equation (A20)

$$\frac{1}{V^2_{\rm nmo}(\mathcal{L})} = \mathcal{L}\,\mathbf{U}\,\mathcal{L}^{\mathbf{T}} \tag{1}$$

as the product of the unit row- and column-vectors $\mathcal{L}$ and $\mathcal{L}^{\mathbf{T}}$, and the 3×3 symmetric matrix $\mathbf{U}$ which has the elements

$$U_{km} = \tau_0(\mathbf{x})\,\frac{\partial^2 \tau_0(\mathbf{x})}{\partial x_k\,\partial x_m} \equiv \tau_0(\mathbf{x})\,\frac{\partial p_k(\mathbf{x})}{\partial x_m}\,, \qquad (k, m = 1, 2, 3)\,. \tag{2}$$

Here $\tau_0(\mathbf{x})$ is the one-way zero-offset traveltime, and $p_k(\mathbf{x})$ are the components of the slowness vector $\mathbf{p}(\mathbf{x}) = [p_1(\mathbf{x}), p_2(\mathbf{x}), p_3(\mathbf{x})]$ at the common midpoint $\mathbf{x}$.

Equation (1) indicates that the function $V_{\rm nmo}(\mathcal{L})$ is a *centered quadratic surface*. The shape of this surface is determined by the eigenvalues of matrix $\mathbf{U}$ which are real because $\mathbf{U}$ is real and symmetric.

Possible shapes of NMO surfaces

To find out which types of NMO surfaces can be expected in seismic exploration, we relate the matrix $\mathbf{U}$ to the 2×2 matrix $\mathbf{W}$ that describes NMO ellipse in a horizontal plane (see, Grechka and Tsvankin, 1998a). Clearly, the NMO ellipse $\mathbf{W}$ can be viewed as the cross-section of the NMO surface $\mathbf{U}$ by the horizontal plane which is specified by $\mathcal{L}_3 = 0$. Denoting components of the unit vector $\mathcal{L}^{\rm hor}$ in the horizontal plane as

$$\mathcal{L}^{\rm hor} = [\cos\alpha,\, \sin\alpha,\, 0]\,, \tag{3}$$

where α is the azimuth of the CMP line, and substituting equation (3) into (1), obtain

$$\frac{1}{V^2_{\rm nmo}(\alpha)} = [\cos\alpha,\, \sin\alpha,\, 0]\,\mathbf{U}\begin{bmatrix}\cos\alpha\\ \sin\alpha\\ 0\end{bmatrix} = U_{11}\cos^2\alpha + 2\,U_{12}\sin\alpha\cos\alpha + U_{22}\sin^2\alpha\,. \tag{4}$$

Comparing this equation with equation (1) in Grechka and Tsvankin (1998a)

$$\frac{1}{V^2_{\rm nmo}(\alpha)} = W_{11}\cos^2\alpha + 2\,W_{12}\sin\alpha\cos\alpha + W_{22}\sin^2\alpha \tag{5}$$

yields

$$U_{ij} = W_{ij} \qquad (i, j = 1, 2)\,. \tag{6}$$

Thus, the matrix $\mathbf{U}$ can be written in the form

$$\mathbf{U} = \begin{pmatrix} W_{11} & W_{12} & U_{13}\\ W_{12} & W_{22} & U_{23}\\ U_{13} & U_{23} & U_{33}\end{pmatrix}\,. \tag{7}$$

This equation allows us to use the known properties of matrix $\mathbf{W}$ (Grechka and Tsvankin, 1998a; Grechka et al., 1999) to make several important observations about the matrix $\mathbf{U}$. First, if we have the NMO ellipse $\mathbf{W}$ measured from data, we need to determine only three quantities U_{k3} to reconstruct the NMO surface $\mathbf{U}$. Below, we show that this can be done by differentiating the Christoffel equation. Second, since the explicit expressions for the elements W_{ij} in homogeneous anisotropic media are known [Grechka et al., 1999, their equation (B-8)], it becomes possible to obtain also *explicit* expressions for the elements of matrix $\mathbf{U}$. Third, as Grechka and Tsvankin (1998a) pointed out, the matrix $\mathbf{W}$ usually (with a few exceptions) represents an ellipse in the horizontal plane. This means that the NMO surfaces $\mathbf{U}$ usually have elliptical cross-sections in the plane $\mathcal{L}_3 = 0$. There are only *three* distinct types of quadratic surfaces with such cross-sections: an *ellipsoid*, an *one sheeted hyperboloid*, and an *elliptical cylinder*. The other types of NMO surfaces (e.g., two sheeted hyperboloid, imaginary elliptical cylinder, hyperbolic cylinder, etc.) are possible only when there is at least one spatial direction where squared NMO velocity is negative and, consequently, reflection traveltime decreases with the offset. Although such shapes of NMO surfaces are not prohibited in the theory, their actual occurrence can be expected to be rare.

Numerical example

It is not difficult to infer from equation (1) that NMO velocity $V_{\rm nmo}$ can be infinite or imaginary in certain directions if the NMO surface is a cylinder or hyperboloid. Therefore a reasonable question may be how often those surfaces can be encountered. Since a comprehensive discussion about NMO cylinders is presented below, here, we give a qualitative answer that the NMO cylinders

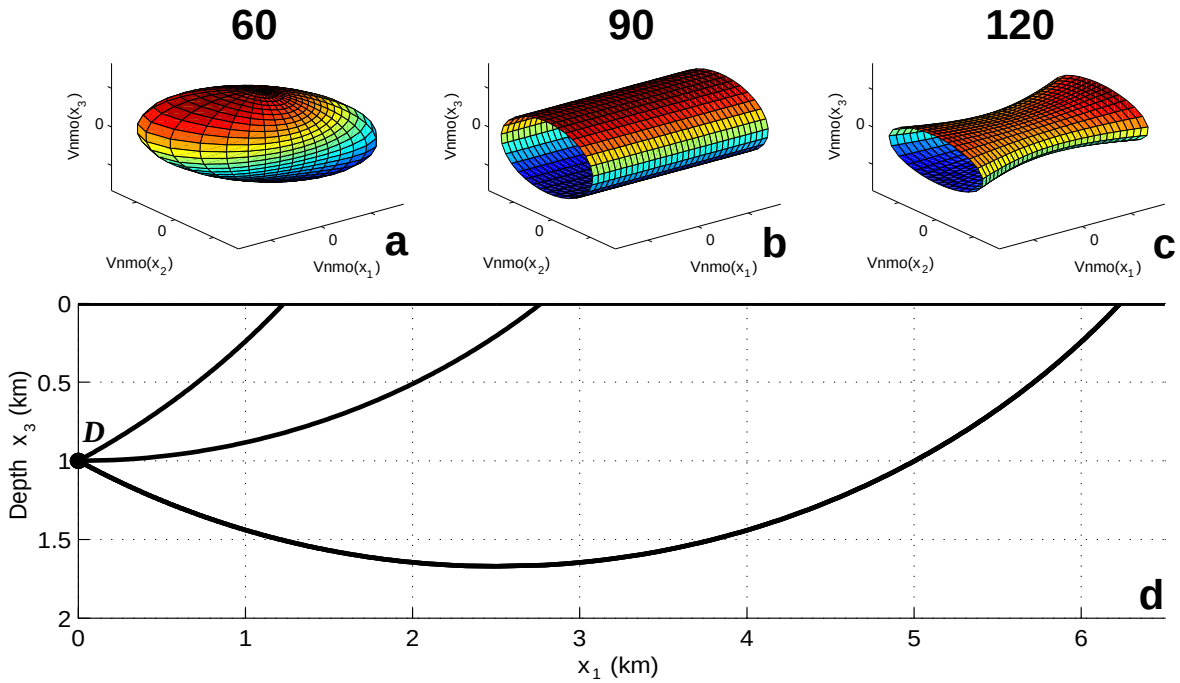

Figure 1. The NMO surfaces (a)–(c) and trajectories of rays (d) excited by a point diffractor D at $[0, 0, 1]$ km in vertically inhomogeneous isotropic medium with constant velocity gradient $V(x_3) = V_0 + \nu x_3$, $V_0 = 2.0$ km/s, $\nu = 0.6$ s^{-1}. The numbers marked on top of Figures (a)–(c) correspond to the dips (in degrees) of imaginary reflectors at D which produce the zero-offset rays shown in Figure (d).

and one sheeted hyperboloids are not uncommon. To illustrate this answer, we computed the NMO surfaces in an isotropic model with constant vertical velocity gradient $V(x_3) = V_0 + \nu x_3$. In this particular model, one-way traveltime $\tau_0(\mathbf{x})$ between the coordinate origin and point $\mathbf{x} = [x_1, x_2, x_3]$ is known analytically (Slotnick, 1959)

$$\tau_0(\mathbf{x}) = \frac{1}{\nu}\,\cosh^{-1}\left[1 + \frac{\nu^2\,(x_1^2 + x_2^2 + x_3^2)}{2\,V_0\,(V_0 + \nu x_3)}\right].$$

Thus, using equation (2), it becomes possible to find explicit expressions for elements of the matrix $\mathbf{U}$. Figure 1 demonstrates the obtained NMO surfaces along with computed ray trajectories which are circular arcs in this case. Clearly, depending on the reflector dip, we can have all the possibilities: ellipsoid, cylinder, and hyperboloid. Numerical tests for other isotropic models where velocity monotonically increases with depth indicate that NMO ellipsoids always correspond to reflector dips below the vertical, NMO cylinders can be obtained only for vertical reflectors*, and hyperboloids are associated with overhanging reflectors.

* It can be proved that for vertical reflectors in *any* isotropic $V(x_3)$ media reflection traveltime is constant, i.e., there is no moveout (Ken Larner, pers. comm.).

Computing NMO surfaces

Inhomogeneous anisotropic media

Although the NMO surface $\mathbf{U}$ is determined by six generally independent quantities [e.g., equation (7)], we show that only *three* NMO velocity measurements are sufficient to reconstruct the whole surface, and the remaining three quantities can be found from the Christoffel equation. Without loss of generality we assume that the directions along which velocity measurements have been made belong to the horizontal plane, so essentially we know the NMO ellipse $\mathbf{W}$ and the zero-offset traveltime τ_0. Differentiating the Christoffel equation written in the form

$$F(\mathbf{p}, \mathbf{x}) = 0\,, \tag{8}$$

where $\mathbf{p}$ and $\mathbf{x}$ are the slowness vector and the spatial coordinates of the zero-offset ray, we obtain the derivatives

$$F_{p_k} \equiv \frac{\partial F}{\partial p_k} \qquad \text{and}$$

$$F_{x_k} \equiv \frac{\partial F}{\partial x_k}\,, \qquad (k = 1, 2, 3)\,. \tag{9}$$

The Christoffel equation (8) depends explicitly on the spatial coordinates $\mathbf{x}$ because the elastic stiffness coefficients c_{ij} are functions of $\mathbf{x}$. Combining derivatives (9),

we arrive to the expression for the NMO surface in the form (7) where the elements U_{k3} are given by [see equations (B7) and (B9) in Appendix B]:

$$U_{j3} = q_{,1} W_{1j} + q_{,2} W_{2j} - \tau_0 \frac{F_{x_j}}{F_q}, \qquad (j = 1, 2),$$

$$U_{33} = q_{,1}^2 W_{11} + 2 q_{,1} q_{,2} W_{12} + q_{,2}^2 W_{22} - \tau_0 \frac{q_{,1} F_{x_1} + q_{,2} F_{x_2} + F_{x_3}}{F_q}. \qquad (10)$$

Here, q is the vertical component of the slowness vector $q \equiv p_3$, $q_{,j} \equiv \partial q / \partial p_j = -F_{p_j}/F_q$, and $F_q \equiv \partial F / \partial p_3$.

Since the values of derivatives with respect to spatial coordinates depend on the particular type of heterogeneity and anisotropy at point $\mathbf{x}$, equations (7) and (10) tell us only that the whole NMO surface $\mathbf{U} = \mathbf{U}(\mathbf{x})$ can be reconstructed from the NMO ellipse $\mathbf{W}(\mathbf{x})$ if we know the *local* values of elastic constants $c_{ij}(\mathbf{x})$ and the slowness vector $\mathbf{p}(\mathbf{x})$.

Homogeneous arbitrary anisotropic media

Since the derivatives F_{x_k} vanish in homogeneous anisotropic media because elastic stiffness coefficients do not vary spatially, the NMO surface $\mathbf{U}^{\rm hom}$, obtained from equations (7) and (10), has the form

$$\mathbf{U}^{\rm hom} = \begin{pmatrix} W_{11} & W_{12} & q_{,1} W_{11} + q_{,2} W_{12} \\ \bullet & W_{22} & q_{,1} W_{12} + q_{,2} W_{22} \\ \bullet & \bullet & q_{,1}^2 W_{11} + 2 q_{,1} q_{,2} W_{12} + q_{,2}^2 W_{22} \end{pmatrix}. \qquad (11)$$

Bullets in the low left-hand corner of the matrix (11) denote the elements equal to their symmetric ones in the upper right-hand corner.

This time, it is instructive to analyze the matrix $\mathbf{U}^{\rm hom}$. Evidently,

$$\det \mathbf{U}^{\rm hom} = 0 \qquad (12)$$

due to the following linear relation between the columns of the matrix $\mathbf{U}^{\rm hom}$:

$$q_{,1}\, U_{k1}^{\rm hom} + q_{,2}\, U_{k2}^{\rm hom} = U_{k3}^{\rm hom}, \qquad (k = 1, 2, 3).$$

Since the first and the second columns are generally independent, the matrix $\mathbf{U}^{\rm hom}$ has exactly one zero eigenvalue. Thus, the NMO surface represented by this matrix is a *cylinder*. When the matrix $\mathbf{W}$ describes an ellipse, the NMO surface $\mathbf{U}^{\rm hom}$ is an *elliptical cylinder*. This conclusion is valid for *any* pure modes in homogeneous *arbitrary* anisotropic media.

Now, we find the direction of the axis of the NMO cylinder. This direction is parallel to eigenvector $\mathbf{e} = [e_1, e_2, e_3]$ which corresponds to zero eigenvalue of the matrix $\mathbf{U}^{\rm hom}$. Solving the eigenvector problem, we obtain from the first two rows of the matrix (11)

$$\begin{cases} W_{11} \frac{e_1}{e_3} + W_{12} \frac{e_2}{e_3} = -q_{,1} W_{11} - q_{,2} W_{12}, \\ W_{12} \frac{e_1}{e_3} + W_{22} \frac{e_2}{e_3} = -q_{,1} W_{12} - q_{,2} W_{22}, \end{cases} \qquad (13)$$

therefore,

$$\frac{e_i}{e_3} = -q_{,i}, \qquad (i = 1, 2). \qquad (14)$$

To reveal the physical meaning of equation (14), we refer to equation (B-3) of Grechka et al. (1999). They derived the relation between components g_k of the group velocity vector $\mathbf{g}$ in exactly the same form:

$$\frac{g_i}{g_3} = -q_{,i}, \qquad (i = 1, 2). \qquad (15)$$

Comparing equations (14) and (15), we see that the axis $\mathbf{e}$ of the NMO cylinder in homogeneous anisotropic media points in the direction of the group velocity vector $\mathbf{g}$ or in the direction of the zero-offset ray. This result becomes less surprising when we relate it to the fact that the NMO velocity is infinite in the direction $\mathbf{e}$. Suppose the we have a CMP line oriented along a fixed straight zero-offset ray. Since the total ray length does not depend on the offset in such a geometry and the medium is homogeneous, the two-way reflection traveltime is also independent of the offset, which is exactly the condition for the NMO velocity to be infinite [see equation (A19)].

To conclude this section, we reproduce the equation for the NMO ellipse $\mathbf{W}$ in terms of the slowness components and their derivatives given by Grechka et al. (1999, their equation (B-8))

$$\mathbf{W} = \frac{p_1 q_{,1} + p_2 q_{,2} - q}{q_{,11} q_{,22} - q_{,12}^2} \begin{pmatrix} q_{,22} & -q_{,12} \\ -q_{,12} & q_{,11} \end{pmatrix}, \qquad (16)$$

where

$$q_{,ij} = -\frac{F_{p_i p_j} + F_{p_i q} q_{,j} + F_{p_j q} q_{,i} + F_{qq} q_{,i} q_{,j}}{F_q}, \qquad (i, j = 1, 2),$$

$F_{p_i p_j} \equiv \partial^2 F / \partial p_i \partial p_j$, $F_{p_i q} \equiv \partial^2 F / \partial p_i \partial q$, and $F_{qq} \equiv \partial^2 F / \partial q^2$. Since all quantities in equation (16) can be obtained explicitly from the Christoffel equation in homogeneous anisotropic media, equations (11) and (16) indicate that the NMO cylinder also can be constructed *analytically* for any given slowness vector $\mathbf{p} = [p_1, p_2, q]$.

Summarizing this section, we conclude that the NMO surface in homogeneous anisotropic media is always an elliptical cylinder with the axis directed along the group velocity vector. We presented explicit equations (11) and (16) to build the NMO cylinder specified by the slowness vector $\mathbf{p}$.

P-wave NMO cylinder in weakly anisotropic VTI layer

It is obvious from equation (11) that if we can measure the NMO cylinder $\mathbf{U}^{\rm hom}$, we should be able to extract the derivatives $q_{,i}$ in addition to the NMO ellipse

W. The derivatives $q_{,i}$ may constrain additional medium parameters compared to those constrained by the NMO ellipse itself, thus, bearing a potential for parameter estimation. In this section, we examine the P-wave NMO cylinder $\mathbf{U}^{\rm VTI}$ from a dipping reflector below a homogeneous VTI layer and show that such a potential, indeed, exists.

To simplify the derivation of matrix $\mathbf{U}^{\rm VTI}$, we assume that anisotropy is weak, i.e., Thomsen's (1986) anisotropic coefficients $|\epsilon| \ll 1$ and $|\delta| \ll 1$; then, we linearize all the expressions in small quantities ϵ and δ. It is instructive to present our results in terms of the zero-dip P-wave NMO velocity $V_{P0,\rm nmo}$, the anellipticity coefficient η, and δ instead of the original set of Thomsen's parameters which includes the vertical P-wave velocity V_{P0}, ϵ, and δ. The reason for this substitution is that P-wave NMO ellipse [i.e., the elements W_{ij} in equation (11) expressed through the horizontal slowness components p_1 and p_2] from a dipping reflector beneath VTI media in known to depend only on

$$V_{P0,\rm nmo} = V_{P0}\,\sqrt{1+2\,\delta} \tag{17}$$

and

$$\eta = \frac{\epsilon-\delta}{1+2\,\delta}\,, \tag{18}$$

and be independent of δ (Grechka and Tsvankin, 1998a).

Selecting the coordinate frame $[x_1, x_2, x_3]$ (Figure 2a) which vertical plane $[x_1, x_3]$ contains the normal to the reflector (the slowness component $p_2 = 0$ in this frame), we obtain the following linearized expressions:

$$U_{11}^{\rm VTI} \equiv W_{11}^{\rm VTI} = \frac{1}{V_{P0,\rm nmo}^2} - p_1^2\,\left[1+2\,\eta\,(4\,y^2-9\,y+6)\right]\,, \tag{19}$$

$$U_{12}^{\rm VTI} \equiv W_{12}^{\rm VTI} = 0\,, \tag{20}$$

$$U_{22}^{\rm VTI} \equiv W_{22}^{\rm VTI} = \frac{1}{V_{P0,\rm nmo}^2} - 2\,\eta\,p_1^2\,(2-y)\,, \tag{21}$$

$$U_{13}^{\rm VTI} = -\frac{p_1\,\sqrt{1-y}}{V_{P0,\rm nmo}}\,\left[1+\delta-\eta\,y\,\frac{8\,y^2-15\,y+8}{1-y}\right]\,, \tag{22}$$

$$U_{23}^{\rm VTI} = 0\,, \tag{23}$$

$$U_{33}^{\rm VTI} = p_1^2\,\left[1+2\,\delta-4\,\eta\,y\,(1-2\,y)\right]\,, \tag{24}$$

where $y = p_1^2\,V_{P0,\rm nmo}^2$.

The first three equations (19)–(21) are known. They describe the NMO ellipse $\mathbf{W}^{\rm VTI}$ recorded in the horizontal plane. The elliptical axes point in the reflector dip and strike directions. Equation (19) represents the dip-component of P-wave NMO velocity [Alkhalifah and Tsvankin, 1995, their equation (A-10)] while equation (21) gives the strike-component [Grechka and Tsvankin, 1998a, their equation (11)]. Clearly, the NMO ellipse $\mathbf{W}^{\rm VTI}$ is independent of δ (at least, in the weak anisotropy approximation).

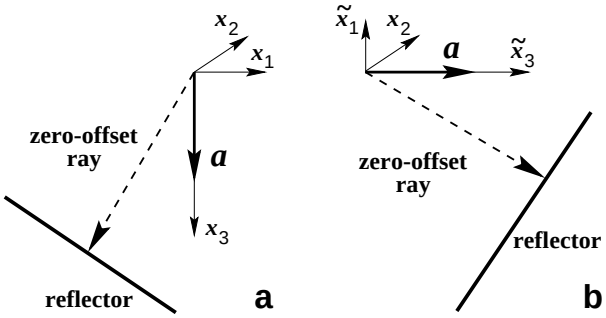

Figure 2. Dipping reflectors beneath VTI (a) and HTI (b) media. HTI model is obtained rotating the VTI one by 90° around coordinate axis x_2. The reflector dip planes are the vertical planes $[x_1, x_3]$ and $[\tilde{x}_1, \tilde{x}_3]$.

Equations (22)–(24) extend the NMO ellipse $\mathbf{W}^{\rm VTI}$ to the NMO cylinder $\mathbf{U}^{\rm VTI}$. In contrast to equations (19)–(21), they indicate that NMO velocities measured along any nonhorizontal direction do depend on δ as well as on $V_{P0,\rm nmo}$ and η. This, seemingly unexpected result, in fact, could have been predicted even before deriving any equations by noting that the vertical symmetry axis **a** in Figure 2a becomes horizontal after rotating the whole plot by 90° around the coordinate axis x_2. This rotation transforms VTI model in Figure 2a into HTI model (transversely isotropic with a horizontal symmetry axis) in Figure 2b. The quantities $U_{22}^{\rm VTI}$ and $U_{33}^{\rm VTI}$, which determine P-wave NMO ellipse in the vertical $[x_2, x_3]$-plane of the original VTI model, describe the NMO ellipse $\mathbf{W}^{\rm HTI}$ in the *horizontal* $[x_2, \tilde{x}_3]$-plane of our new HTI model. The ellipse $\mathbf{W}^{\rm HTI}$, as proven by Contreras et al. (1999), constrains both anisotropic coefficients η and δ (or ϵ and δ) individually. It also can be shown that our equations (21), (23), and (24) represent the NMO ellipse derived by Contreras et al. (1999, their equations (22) and (32)) in terms of anisotropic coefficients $\eta^{(\rm V)}$ and $\delta^{(\rm V)}$ introduced by Tsvankin (1997) and Rüger (1997) to describe seismic signatures in HTI media.

It may seem from the presented discussion that P-wave NMO velocities measured within a horizontal plane do not provide sufficient information for estimating both values of ϵ and δ in VTI media. While this is correct for a single VTI layer, we will show that the presence of lateral heterogeneity (such as intermediate dipping interfaces) in the subsurface may help to obtain those anisotropic coefficients using surface P-wave reflection data alone.

Dix-type formulae in inhomogeneous anisotropic media

The above described NMO surfaces $\mathbf{U}(\mathbf{x})$ can be called the "effective" NMO surfaces because they incorporate

the influence of medium along the whole ray path between the reflection point and the CMP location $\mathbf{x}$. Here, we look at the NMO surfaces from a different perspective and show that the very definition (2) of the matrix $\mathbf{U}$ can be used to devise the Dix-type formulae to build the "effective" NMO surfaces from the interval (or local) ones in *heterogeneous* anisotropic media.

General considerations

Let us begin with rewriting equation (2) in the vector form

$$\mathbf{U} = \tau_0 \frac{\partial \mathbf{p}}{\partial \mathbf{x}},$$

or

$$\tau_0 \, \mathbf{U}^{-1} = \frac{\partial \mathbf{x}}{\partial \mathbf{p}}. \tag{25}$$

Now, suppose that a combination of components p_k of the slowness vector $\mathbf{p}$ is preserved in some plane $\mathcal{P}$ along a segment L of the zero-offset ray. Constructing a cross-section of the NMO surface $\mathbf{U}$ by the plane $\mathcal{P}$, we obtain the NMO ellipse

$$\mathbf{W}^{\mathcal{P}} = \mathbf{U} \bigcap \mathcal{P}.$$

Then, equation (25) can be written for the cross-section $\mathbf{W}^{\mathcal{P}}$:

$$\tau_0 \, \left[\mathbf{W}^{\mathcal{P}}\right]^{-1} = \left.\frac{\partial \mathbf{x}}{\partial \mathbf{p}}\right|_{\mathbf{p}\in\mathcal{P}}. \tag{26}$$

Next, assume that the segment L is subdivided into a number of smaller intervals ℓ, and the interval zero-offset traveltimes $\tau_{0,\ell}$ and the NMO ellipses $\mathbf{W}^{\mathcal{P}}_{\ell}$ are defined at each interval. We can repeat the derivation in Appendix A for any given interval ℓ and show that $\tau_{0,\ell}$ and $\mathbf{W}^{\mathcal{P}}_{\ell}$ relate to the interval ray coordinates $\mathbf{x}_\ell$ by equation similar to (26), namely,

$$\tau_{0,\ell} \, \left[\mathbf{W}^{\mathcal{P}}_{\ell}\right]^{-1} = \left.\frac{\partial \mathbf{x}_\ell}{\partial \mathbf{p}}\right|_{\mathbf{p}\in\mathcal{P}}. \tag{27}$$

Note that the slowness components here are the same as those in equation (26) because we assumed that they are preserved along the whole ray segment L. Since due to the ray continuity

$$\mathbf{x} = \sum_\ell \mathbf{x}_\ell \quad \text{and} \quad \tau_0 = \sum_\ell \tau_{0,\ell}, \tag{28}$$

equations (26) and (27) lead to

$$\left[\mathbf{W}^{\mathcal{P}}\right]^{-1} = \frac{\sum_\ell \tau_{0,\ell} \, \left[\mathbf{W}^{\mathcal{P}}_{\ell}\right]^{-1}}{\sum_\ell \tau_{0,\ell}}. \tag{29}$$

Equation (29) represents the Dix-type averaging formula which is very similar to that obtained by Grechka et al. (1999) for the NMO ellipses $\mathbf{W}$ in the horizontal plane $[x_1, x_2]$. The difference, however, is that now the Dix-type formula has been derived for an *arbitrary* plane $\mathcal{P}$, not necessarily for $\mathcal{P} = [x_1, x_2]$. Still, we have made the assumption that the projection of the slowness vector $\mathbf{p}$ onto $\mathcal{P}$ is preserved along the whole ray segment L for which the Dix-type formula (29) has been obtained.

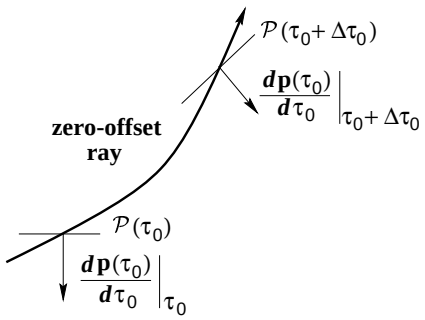

Figure 3. The projection of the slowness vector $\mathbf{p}(\tau_0)$ onto the plane $\mathcal{P}(\tau_0) \perp d\mathbf{p}/d\tau_0$ is locally preserved even if the medium is inhomogeneous and anisotropic.

Arbitrary heterogeneity and anisotropy

As one may infer from the previous section, the important condition for deriving the Dix-type formulae is the conservation of certain components of the slowness vector. In fact, equations (2), (7), and (10) for the NMO surfaces $\mathbf{U}$ allow obtaining the Dix-type formulae even when *neither one* slowness component is preserved, i.e., in arbitrary heterogeneous anisotropic media.

We begin with equations for zero-offset ray in inhomogeneous anisotropic media:

$$\frac{d\mathbf{x}}{d\tau_0} = \frac{\partial H}{\partial \mathbf{p}} \qquad \text{and} \qquad \frac{d\mathbf{p}}{d\tau_0} = -\frac{1}{2}\frac{\partial H}{\partial \mathbf{x}}, \tag{30}$$

where τ_0 is the traveltime along the ray, and particular form of the Hamiltonian $H \equiv H(\mathbf{p}, \mathbf{x})$ is not important here (see, e.g., Červeny et al., 1977). The second equation (30) explicitly indicates that the slowness $\mathbf{p}$ changes *only* along the vector $d\mathbf{p}/d\tau_0$ as we move along the ray. As the consequence of this fact, one can *always* find a plane $\mathcal{P}(\tau_0)$, specifically $\mathcal{P}(\tau_0) \perp d\mathbf{p}/d\tau_0$, where the slowness components are *locally preserved* (Figure 3). Therefore, we can apply equation (29) to the cross-section

$$\mathbf{W}^{\mathcal{P}(\tau_0)}(\tau_0) = \mathbf{U}(\tau_0) \bigcap \mathcal{P}(\tau_0)$$

of the NMO surface $\mathbf{U}(\tau_0)$ by the plane $\mathcal{P}(\tau_0)$ at the infinitesimal ray segment specified by the traveltime $\Delta\tau_0$. This results in the cross-section $\mathbf{W}^{\mathcal{P}(\tau_0)}(\tau_0+\Delta\tau_0)$ of the NMO surface $\mathbf{U}(\tau_0+\Delta\tau_0)$ by the same plane $\mathcal{P}(\tau_0)$.

At traveltime $\tau_0 + \Delta\tau_0$, the plane $\mathcal{P}(\tau_0 + \Delta\tau_0)$, being orthogonal to the vector $d\mathbf{p}/d\tau_0\big|_{\tau_0+\Delta\tau_0}$, is generally different from $\mathcal{P}(\tau_0)$ as schematically shown in Figure 3. To account for that, we reconstruct the NMO surface $\mathbf{U}(\tau_0 + \Delta\tau_0)$ from its cross-section $\mathbf{W}^{\mathcal{P}(\tau_0)}(\tau_0 + \Delta\tau_0)$

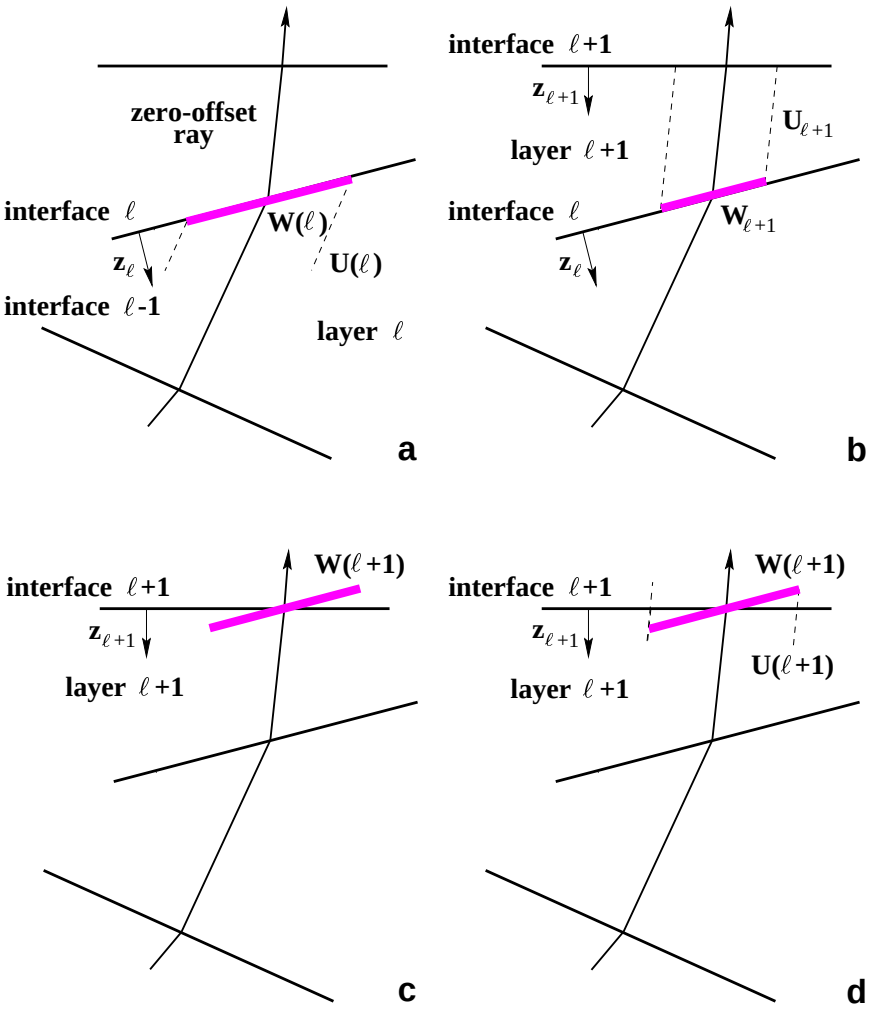

Figure 4. To apply the Dix-type averaging of NMO cylinders in the model that contains homogeneous anisotropic layers separated by plane dipping interfaces, we continue the cross-sections of the cylinders by the interfaces through the layers. The "effective" cross-section $\mathbf{W}(\ell)$ (a) at the top of the ℓth layer and the interval cross-section $\mathbf{W}_{\ell+1}$ (b) in the $\ell+1$th layer are averaged using equation (32) to produce the "effective" cross-section $\mathbf{W}(\ell+1)$ (c) of the NMO cylinder $\mathbf{U}(\ell+1)$ (d) by the plane parallel to the ℓth interface.

and, then, make another cross-section of $\mathbf{U}(\tau_0+\Delta\tau_0)$ by the plane $\mathcal{P}(\tau_0+\Delta\tau_0)$:

$$\mathbf{W}^{\mathcal{P}(\tau_0+\Delta\tau_0)}(\tau_0+\Delta\tau_0)=\mathbf{U}(\tau_0+\Delta\tau_0)\bigcap\mathcal{P}(\tau_0+\Delta\tau_0).$$

This completes the process, and the cross-section $\mathbf{W}^{\mathcal{P}(\tau_0+\Delta\tau_0)}(\tau_0+\Delta\tau_0)$ can be continued along the next time interval $[\tau_0+\Delta\tau_0,\ \tau_0+2\Delta\tau_0]$. The mathematics and details of the whole procedure are given in Appendixes C and D.

Special case: homogeneous anisotropic layers separated by plane interfaces

The developed theory of Dix-type averaging of NMO surfaces can be applied to an important special case – the model that consists of several homogeneous anisotropic layers separated by plane arbitrarily dipping interfaces (Figure 4). In this model, projections of the slowness vectors onto the interfaces are preserved due to Snell's law, i.e.,

$$\mathbf{p}_\ell\times\mathbf{z}_\ell=\mathbf{p}_{\ell+1}\times\mathbf{z}_\ell \tag{31}$$

at ℓth interface with the unit normal $\mathbf{z}_\ell$ (Figure 4). Therefore, the model interfaces play the role of the above discussed planes $\mathcal{P}(\tau_0)$ which determine the cross-sections of the NMO surfaces $\mathbf{U}$ to be continued.

Since all necessary equations have already been derived, here, we summarize the process of constructing the NMO surfaces which become the cylinders because the layers are homogeneous. Figure 4 schematically illus-

trates our procedure in 2-D. We assume that the slownesses $\mathbf{p}_\ell$ and traveltimes $\tau_{0,\ell}$ have already been obtained from ray tracing. The Dix-type averaging includes the following steps:

Step 1. To begin, compute the NMO cylinder $\mathbf{U}_1$ in the layer $\ell = 1$ immediately above the reflector. Use equations (11) and (16) for the slowness vector $\mathbf{p}_1$ which is parallel to the reflector normal $\mathbf{z}_0$. The interval NMO cylinder $\mathbf{U}_1$ is equal to the "effective" cylinder $\mathbf{U}(1)$ in the first layer. If the layer number $\ell > 1$, the cylinder $\mathbf{U}(\ell)$ (dashed lines in Figure 4a) is known after continuation from below.

Step 2. Apply equation (D7) to determine the cross-section $\mathbf{W}(\ell)$ (gray line in Figure 4a) of the cylinder $\mathbf{U}(\ell)$ by the ℓth interface.

Step 3. Compute the interval NMO cylinder $\mathbf{U}_{\ell+1}$ (dashed lines in Figure 4b) using equations (11) and (16) for the slowness vector $\mathbf{p}_{\ell+1}$. Find the cross-section $\mathbf{W}_{\ell+1}$ (gray line in Figure 4b) of the cylinder $\mathbf{U}_{\ell+1}$ by the ℓth interface with the normal $\mathbf{z}_\ell$.

Step 4. Obtain the "effective" cross-section $\mathbf{W}(\ell+1)$ at the top of the $\ell+1$th layer (gray line in Figure 4c) applying the Dix-type averaging formula (C1):

$$[\mathbf{W}(\ell+1)]^{-1} = \frac{\tau_0(\ell)\ [\mathbf{W}(\ell)]^{-1} + \tau_{0,\ell+1}\ [\mathbf{W}_{\ell+1}]^{-1}}{\tau_0(\ell+1)}, \qquad (32)$$

where $\tau_0(\ell) = \sum_{j=1}^{\ell} \tau_{0,j}$.

Step 5. Reconstruct the NMO cylinder $\mathbf{U}(\ell+1)$ (dashed lines in Figure 4d) using equations (D12) and (11).

Step 6. Repeat **Step 2** for the next $\ell+1$th layer.

The described sequence allows one to apply the Dix-type procedure in the stripping mode. Suppose we have measured at some plane $\mathcal{P}$ the NMO ellipses $\mathbf{W}^{\mathcal{P}}(\ell+1)$ and $\mathbf{W}^{\mathcal{P}}(\ell)$ corresponding to reflections from the $\ell+1$th and ℓth interfaces. Then, the following algorithm can be proposed for obtaining the interval NMO cylinder $\mathbf{U}_{\ell+1}$:

Step 1. Compute the slowness vector $\mathbf{p}_{\ell+2}$ which corresponds to the ray segment immediately above the $\ell+1$th interface of the ray reflected from the deeper ℓth interface. Then, use equation (D12), which is needed if $\mathcal{P} \neq [x_1, x_2]$, and equation (11) to reconstruct the cylinders $\mathbf{U}(\ell+1)$ and $\mathbf{U}(\ell)$. Naturally, these cylinders correspond to different slowness vectors, namely, to the computed vector $\mathbf{p}_{\ell+2}$ and to vector $\mathbf{p}_{\ell+1}$; the latter is parallel to the normal $\mathbf{z}_\ell$ of ℓth interface.

Step 2. Apply equation (D7) to determine the cross-sections $\mathbf{W}(\ell+1)$ and $\mathbf{W}(\ell)$ of the cylinders $\mathbf{U}(\ell+1)$ and $\mathbf{U}(\ell)$ by the $\ell+1$th interface.

Step 3. Find the cross-section $\mathbf{W}_{\ell+1}$ of interval NMO cylinder $\mathbf{U}_{\ell+1}$ by the $\ell+1$th interface:

$$[\mathbf{W}_{\ell+1}]^{-1} = \frac{\tau_0(\ell)\ [\mathbf{W}(\ell)]^{-1} - \tau_0(\ell+1)\ [\mathbf{W}(\ell+1)]^{-1}}{\tau_0(\ell) - \tau_0(\ell+1)}. \qquad (33)$$

Step 4. Reconstruct the interval NMO cylinder $\mathbf{U}_{\ell+1}$ using equation (11) and equation (D12); the latter equation is needed if the $\ell+1$th interface is not horizontal.

This stripping procedure, clearly, requires knowledge of anisotropic parameters, and actual dip and depth of the $\ell+1$th interface. Although it is beyond the scope of our paper to discuss in detail how to get those parameters from seismic data, below, we point out some potential possibilities.

Numerical example

To show that the Dix-type averaging produces correct results in anisotropic layered media, we computed the P-wave NMO ellipses at the surface $x_3 = 0$ in a model containing three TTI layers (transversely isotropic with a tilted symmetry axis). The model parameters are given in Table 1. Figure 5 displays the ellipse computed using the Dix-type averaging procedure (solid) along with that reconstructed from traveltimes computed numerically along six CMP lines (dotted). The ellipses almost coincide indicating that the Dix-type averaging formula is correct. The small difference up to 1.6% between the solid and dotted ellipses in Figure 5 can be attributed to the influence of nonhyperbolic moveout which is not taken into account by our NMO equations. However, as Figure 5 illustrates, the errors due to nonhyperbolic moveout are small when maximum offset is equal to the distance between the common midpoint and the reflector. The same conclusion holds for a wide variety of anisotropic models (e.g., Tsvankin and Thomsen, 1994; Tsvankin, 1995; Grechka and Tsvankin, 1999a).

Potential for anisotropic parameter estimation

Let us relate two important results:

1. The Dix-type averaging and differentiation of NMO surfaces $\mathbf{U}$ operates with the cross-sections $\mathbf{W}^{\mathcal{P}}$ of those surfaces by generally *nonhorizontal* planes $\mathcal{P}$ which are determined by either derivatives of the slowness vectors $d\mathbf{p}/d\tau_0$ (Figure 3) or dipping interfaces (Figure 4).
2. The cross-sections $\mathbf{W}^{\mathcal{P}} = \mathbf{U} \bigcap \mathcal{P}$ may depend on anisotropic parameters which are not constrained by NMO ellipses $\mathbf{W}^{[x_1,x_2]} = \mathbf{U} \bigcap [x_1, x_2]$ in a horizontal plane as it happened for P-waves in VTI media [equations (19)–(24)].

Thus, we can infer that certain types of lateral heterogeneity, which is needed to make the planes $\mathcal{P}$ non-

Depth (km)	V_{P0} (km/s)	ϵ	δ	ν	β	ϕ_1	ϕ_2
1.0	0.5	0.20	0.10	10	60	20	20
2.0	1.0	0.10	0.07	20	50	40	60
3.0	2.0	0.15	0.10	30	40	30	0

Table 1. Relevant parameters of TTI model with dipping intermediate interfaces. The tilts ν and azimuths β of the of the symmetry axes as well as reflector dips ϕ_1 and azimuths ϕ_2 are given in degrees.

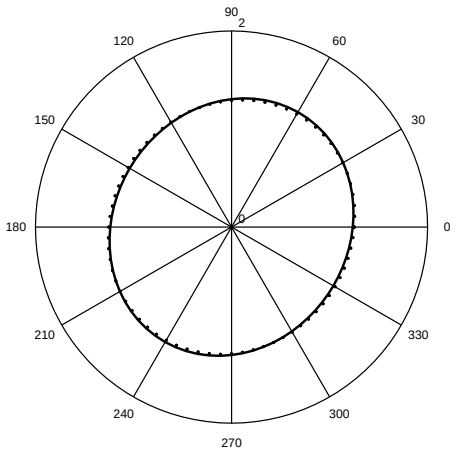

Figure 5. NMO ellipses computed for P-wave reflection from the deepest reflector in TTI model with parameters from Table 1. Solid – the ellipse obtained using the Dix-type procedure; dotted – reconstructed from ray-traced traveltimes computed along six azimuths with 30° separation up to maximum offset $X = 3$ km equal to the reflector depth.

horizontal, may actually aid estimating of anisotropic parameters. For example, the presence of intermediate dipping interfaces in the above examined VTI model produces the cross-sections $\mathbf{W}^{\mathcal{P}}$ of P-wave NMO surfaces which depend on the vertical P-wave velocity, and Thomsen's anisotropic coefficients ϵ and δ. Then, those cross-sections appear in the Dix-type averaging formula causing dependence of the "effective" NMO ellipse on *interval* values of the vertical velocity, ϵ, and δ. Knowing the vertical velocity enables one to perform *depth* processing in VTI media based solely on surface P-wave data. Note that this possibility does not exist in laterally homogeneous VTI media where P-wave reflection data provide information only for *time* processing (Alkhalifah and Tsvankin, 1995).

The presented discussion indicates that, depending on type of lateral heterogeneity, P-wave reflection traveltimes may contain sufficient information for depth processing in anisotropic media. We will describe one such example in a sequel paper. The presence of irregular interfaces, causing wide angular distribution of reflected rays, may also aid anisotropic parameter estimation in depth and even allow one to attempt doing anisotropic reflection tomography of one sort or another. The increased subsurface complexity, on the other hand, may produce various trade-offs between anisotropy and the structure of interfaces. Examining those trade-offs and finding the cases when they can be overcome opens a new area of anisotropic velocity analysis based on understanding of NMO surfaces.

Discussion and Conclusions

The paper contains two main parts: derivation of NMO surfaces $\mathbf{U}$ in inhomogeneous arbitrary anisotropic media and establishing the Dix-type procedure to integrate (or average) and differentiate (or strip) the NMO surfaces along zero-offset rays. The developed theory is geometrical by its nature. Realizing that the surfaces $\mathbf{U}$ belong to the class of *centered quadratic* surfaces for *any* model has allowed us to use the well-known methods developed in analytical geometry to represent the surfaces by symmetric 3×3 matrices U_{km} and perform all operations with NMO surfaces discussed in the paper. For example, we have shown how to compute the NMO surfaces, find their cross-sections, and reconstruct the surfaces from the cross-sections back. These operations constitute the mathematics which is needed for the Dix-type averaging and differentiation of the NMO surfaces.

Although mathematical treatment of surfaces $\mathbf{U}$ may be interesting by itself, geophysical results, which come from the theory we have developed, are more important because analysis of NMO velocities lies in the heart of seismic processing. Here, we discuss some of those results. The immediate consequence of the fact the surface $\mathbf{U}$ is quadratic is that it depends on *six* generally independent quantities U_{km} ($k \le m$, $m = 1, 2, 3$) which all, in principle, can be measured from data. Since we have shown how those quantities relate to elastic parameters of the model, the NMO velocity measurements can be inverted for the model parameters. As we have illustrated for a simple homogeneous VTI model, such measurements do constrain anisotropic coefficients which otherwise cannot be estimated. It is also important to emphasize that the NMO surfaces are built both from quantities which are averaged between CMP location and reflection point and from *local* quantities at the common midpoint. This becomes evident from analyzing equations (7) and (10): if we assume lateral homogeneity, matrix $\mathbf{W}$ expresses the "effective" NMO ellipse whereas the derivatives of q and F refer to quantities related by the Christoffel equation at the midpoint. For this reason, for instance, the surface $\mathbf{U}$ is always going to be a

cylinder if medium is homogeneous at the midpoint [see equation (11)] regardless the structure of the subsurface below.

The surfaces **U** provide the most general description of NMO velocities merely because, knowing **U**, we can compute NMO velocity along *any* direction in 3-D space and along any set of directions. One practically important example is given by NMO ellipse which can be treated as a suite of NMO velocities in all directions within a certain plane. On the other hand, NMO ellipse can be viewed as a cross-section of the NMO surface **U** by a plane and, therefore, all properties of NMO ellipses, which were examined in detail by Grechka and Tsvankin (1998a), are derivable from the surfaces **U**. Similarly, the other known properties of NMO velocities are contained in the surfaces **U** and, because of this, the NMO surfaces allow one to relate those properties and possibly establish new ones that may be hidden on a less general level.

The example of such properties, which has been discussed extensively in the paper, is the Dix-type formulae for averaging and differentiating the NMO surfaces. We had to examine the *full* surface **U** in 3-D to show that always, even in the most general inhomogeneous anisotropic media, there is the cross-section of **U** which, at least locally, can be averaged or stripped in the Dix-type manner. It is important to note that other cross-sections of the NMO surface, for which the Dix-type procedure is not applicable, as well as the whole surface **U** can be reconstructed *after* each Dix-type continuation or differentiation step has been applied. This is exactly the reason why our procedure does *not* require any slowness components to be preserved along zero-offset rays as opposed to more conventional generalizations of the famous Dix (1955) formula. Although there is an alternative way of building the NMO velocities and NMO ellipses in heterogeneous media using continuation of the wavefront curvatures (e.g., Hubral and Krey, 1980; Goldin, 1986; Grechka et al., 1999), the existing algorithms utilizing this approach are cumbersome and not that geometrically intuitive compared to the proposed technique which relies on the NMO surfaces.

We have presented a detailed study of the Dix-type averaging and differentiation in a model which contains a set of homogeneous anisotropic layers separated by plane arbitrarily dipping interfaces. Clearly, the Dix-type averaging becomes a purely analytical procedure as soon as the zero-offset ray is found. This procedure involves solving three simultaneous linear equations and manipulating the quantities obtained from ray tracing. Likewise, the Dix-type differentiation in this model is a semi-analytical procedure which, in addition, requires solving the Christoffel equation. To perform the Dix-type averaging or stripping, one generally has to specify the model *in depth*, thus, making the procedure described here a convenient tool for anisotropic parameter estimation. Examining the P-wave NMO cylinders in VTI media, we showed that the presence of intermediate dipping interfaces in the subsurface causes dependence of the "effective" NMO ellipses on both anisotropic coefficients ϵ and δ which are not constrained in laterally homogeneous VTI models. This result indicates potential applications of the theory developed in the paper to anisotropic velocity analysis in *depth* domain with possible further extensions to anisotropic reflection tomography.

Acknowledgments

We are grateful to members of A(nisotropy)-team of the Center for Wave Phenomena (CWP), Colorado School of Mines, for helpful discussions. The support for this work was provided by the members of the Consortium Project on Seismic Inverse Methods for Complex Structures at CWP and by the United States Department of Energy (award #DE-FG03-98ER14908).

References

Alkhalifah, T., and Tsvankin, I., 1995, Velocity analysis in transversely isotropic media: Geophysics, **60**, 1550–1566.

Contreras, P., Grechka, V., and Tsvankin, I., 1999, Moveout inversion of P-wave data for horizontal transverse isotropy: Geophysics, in print.

Červeny, V., Molotkov, I.A., and Pšenčik, I., 1977, Ray method in seismology: Univ. of Karlova.

Chernyak, V.S., and Gritsenko, S.A., 1979, Interpretation of effective parameters of the CDP-method for system of 3-D homogeneous layers separated by irregular interfaces: Geology and Geophysics, **12**, 112–120 (in Russian).

Corrigan, D., Withers, R., Darnall, J., and Skopinski, T., 1996, Fracture mapping from azimuthal velocity analysis using 3D surface seismic data: 66th Ann. Internat. Mtg., Soc. Expl. Geophys., Expanded Abstracts, 1834–1837.

Dix C.H. 1955, Seismic velocities from surface measurements: Geophysics, **20**, 68–86.

Goldin, S.V., 1986, Seismic traveltime inversion: Soc. Expl. Geophys.

Grechka, V., and Tsvankin, I., 1998a, 3-D description of normal moveout in anisotropic media: Geophysics, **63**, 1079–1092.

Grechka, V., and Tsvankin, I., 1998b, Inversion of azimuthally dependent NMO velocity in transversely isotropic media with a tilted axis of symmetry: 68th Ann. Internat. Mtg., Soc. Expl. Geophys., 1483–1486.

Grechka, V., and Tsvankin, I., 1999a, 3-D moveout veloc-

ity analysis and parameter estimation for orthorhombic media: Geophysics, in print.

Grechka, V., and Tsvankin, I., 1999b, 3-D moveout inversion in azimuthally anisotropic media with lateral velocity variation: Theory and a case study: Geophysics, in print.

Grechka, V., Tsvankin, I., and Cohen, J.K., 1999, Generalized Dix equation and analytic treatment of normal-moveout velocity for anisotropic media: Geophysical Prospecting, **47**, 117–148.

Hubral, P., and Krey, T., 1980, Interval velocities from seismic reflection measurements: Soc. Expl. Geophys.

Rüger, A., 1997, P-wave reflection coefficients for transversely isotropic models with vertical and horizontal axis of symmetry: Geophysics, **62**, 713–722.

Slotnick, M.M., 1959, Lessons in seismic computing: Soc. Expl. Geophys.

Thomsen, L., 1986, Weak elastic anisotropy: Geophysics, **51**, 1954–1966.

Tsvankin, I., 1995, Normal moveout from dipping reflectors in anisotropic media: Geophysics, **60**, 268–284.

Tsvankin, I., 1997, Reflection moveout and parameter estimation for horizontal transverse isotropy: Geophysics, **62**, 614–629.

Tsvankin, I., and Thomsen, L., 1994, Nonhyperbolic reflection moveout in anisotropic media: Geophysics, **59**, 1290–1304.

APPENDIX A: Derivation of the NMO velocity

In this appendix, following the general line of Hubral and Krey (1980), Goldin (1986), and Grechka and Tsvankin (1998a), we derive the short-offset approximation of the squared reflection traveltime t^2 recorded at the CMP line oriented along the unit vector $\mathcal{L}$. The idea of the derivation is to expand the traveltime $t(h)$ in Taylor series with respect to the half source-receiver offset h in the vicinity of the zero offset $h = 0$. As it is usually done, we assume the existence of all derivatives which appear in the derivation.

Let us denote $\mathbf{x}$ the coordinate of common midpoint O, and $\mathbf{x} - \mathbf{h}$ and $\mathbf{x} + \mathbf{h}$ the coordinates of the source S and receiver R respectively (Figure A1), and

$$\mathbf{h} \equiv [h_1,\, h_2,\, h_3] = h\mathcal{L} \equiv h\,[\mathcal{L}_1,\, \mathcal{L}_2,\, \mathcal{L}_3]\,. \tag{A1}$$

The pure-mode two-way reflection traveltime t, which depends on positions of the source and receiver, and on coordinate $\mathbf{r}$ of the reflection point, can be represented as a sum of two one-way traveltimes τ corresponding to down- and upgoing rays:

$$t(\mathbf{x}, \mathbf{h}, \mathbf{r}(\mathbf{x}, \mathbf{h})) = \tau(\mathbf{x} - \mathbf{h}, \mathbf{r}) + \tau(\mathbf{x} + \mathbf{h}, \mathbf{r})\,. \tag{A2}$$

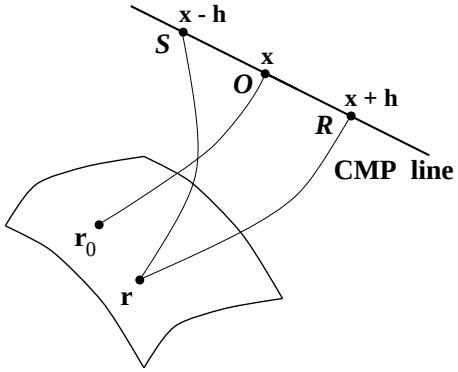

Figure A1. In the derivation of NMO surface, we take into account the fact that the reflection point $\mathbf{r}_0$ of the zero-offset ray does not coincide with the reflection point $\mathbf{r}$ of the nonzero-offset ray.

At the zero offset ($\mathbf{h} = \mathbf{0}$), the traveltime (A2) becomes

$$t(\mathbf{x}, \mathbf{0}, \mathbf{r}_0) \equiv t_0 = 2\,\tau(\mathbf{x}, \mathbf{r}_0) \equiv 2\,\tau_0(\mathbf{x})\,, \tag{A3}$$

where $\mathbf{r}_0 = \mathbf{r}(\mathbf{x}, \mathbf{0})$ is the reflection coordinate of the zero-offset ray (Figure A1) and τ_0 is the one-way zero-offset traveltime.

Now, we calculate the first and second derivatives of the traveltime (A2) with respect half-offset h and evaluate those derivatives at the zero offset. Differentiating equation (A2) yields

$$\frac{dt}{dh} = \sum_{k=1}^{3} \frac{\partial t}{\partial h_k}\,\mathcal{L}_k + \frac{\partial t}{\partial r_k}\,\frac{dr_k}{dh}\,. \tag{A4}$$

Since the coordinate $\mathbf{r}$ of the reflection point can be considered as a parameter of the ray trajectory, Fermat's principle requires that

$$\frac{\partial t}{\partial r_k} = 0\,, \qquad (k = 1, 2, 3)\,, \tag{A5}$$

and equation (A4) takes the form

$$\frac{dt}{dh} = \sum_{i=k}^{3} \frac{\partial t}{\partial h_k}\,\mathcal{L}_k\,. \tag{A6}$$

Using equation (A2), we evaluate the derivative (A6) at the zero offset

$$\left.\frac{dt}{dh}\right|_{h=0} = \sum_{k=1}^{3} \left[-\frac{\partial \tau(\mathbf{x}, \mathbf{r}_0)}{\partial h_k} + \frac{\partial \tau(\mathbf{x}, \mathbf{r}_0)}{\partial h_k}\right] \mathcal{L}_k = 0\,. \tag{A7}$$

Differentiating equation (A6) again yields

$$\frac{d^2t}{dh^2} = \sum_{k,m=1}^{3} \frac{\partial^2 t}{\partial h_k\,\partial h_m}\,\mathcal{L}_k\,\mathcal{L}_m + \frac{\partial^2 t}{\partial h_k\,\partial r_m}\,\frac{dr_m}{dh}\,\mathcal{L}_k\,. \tag{A8}$$

To evaluate the derivative (A8) at $h = 0$, we note that neither traveltime nor ray trajectory changes for a pure reflection mode if we interchange the positions of the

source and receiver (the reciprocity principle) which implies that

$$\mathbf{r}(\mathbf{x}, h\mathcal{L}) = \mathbf{r}(\mathbf{x}, -h\mathcal{L})\,, \tag{A9}$$

i.e., $\mathbf{r}$ is an even function of h and, therefore,

$$\left.\frac{d\mathbf{r}}{dh}\right|_{h=0} = 0\,. \tag{A10}$$

Thus, combining equations (A2), (A8), and (A10), we obtain

$$\left.\frac{d^2t}{dh^2}\right|_{h=0} = \sum_{k,m=1}^{3} \left.\frac{\partial^2 t}{\partial h_k\,\partial h_m}\right|_{h=0} \mathcal{L}_k\,\mathcal{L}_m$$
$$= 2\sum_{k,m=1}^{3} \frac{\partial^2 \tau_0(\mathbf{x})}{\partial x_k\,\partial x_m}\,\mathcal{L}_k\,\mathcal{L}_m\,. \tag{A11}$$

This equation can be viewed as the extension to arbitrarily oriented CMP lines of the well-known normal incidence point (NIP) theorem which was proven by Chernyak and Gritsenko (1979) [their proof can be also found in Goldin (1986)], and by Hubral and Krey (1980). Equation (A11) relates the second-order derivative of the two-way traveltime t with respect to the offset and the partial second-order spatial derivatives of the one-way traveltime τ_0 along the zero-offset ray. Since the derivatives of only *zero-offset* traveltime τ_0 present in equation (A11), we arrive to the known conclusion that reflection point dispersal (i.e., the difference of $\mathbf{r}$ from $\mathbf{r}_0$) can be ignored in deriving the derivative $d^2t/dh^2\,\big|_{h=0}$ and, consequently, in deriving the normal-moveout velocity.

To obtain the equation for NMO velocity along the CMP line $\mathcal{L}$, we expand traveltime t in Taylor series with respect to h in the vicinity of the zero offset

$$t(h,\mathcal{L}) = t(0,\mathcal{L}) + \left.\frac{dt}{dh}\right|_{h=0} h + \left.\frac{d^2t}{dh^2}\right|_{h=0} \frac{h^2}{2} + \ldots\,, \tag{A12}$$

or, using equations (A3), (A7), and (A11),

$$t(h,\mathcal{L}) = t_0 + h^2 \sum_{k,m=1}^{3} \frac{\partial^2 \tau_0(\mathbf{x})}{\partial x_k\,\partial x_m}\,\mathcal{L}_k\,\mathcal{L}_m + \ldots \tag{A13}$$

Squaring equation (A13) and keeping the terms up to quadratic with respect to h yields

$$t^2(h,\mathcal{L}) = t_0^2 + 2\,t_0\,h^2 \sum_{k,m=1}^{3} \frac{\partial^2 \tau_0(\mathbf{x})}{\partial x_k\,\partial x_m}\,\mathcal{L}_k\,\mathcal{L}_m\,. \tag{A14}$$

Introducing the offset

$$X = 2\,h\,, \tag{A15}$$

we rewrite equation (A14) in its final form

$$t^2(X,\mathcal{L}) = t_0^2 + (\mathcal{L}\,\mathbf{U}\,\mathcal{L}^{\mathbf{T}})\,X^2\,, \tag{A16}$$

where $\mathbf{T}$ denotes transposition, and the 3×3 symmetric matrix $\mathbf{U}$ has the components

$$U_{km} = \tau_0\,\frac{\partial^2 \tau_0(\mathbf{x})}{\partial x_k\,\partial x_m} \equiv \tau_0\,\frac{\partial p_k(\mathbf{x})}{\partial x_m}\,, \qquad (k,m=1,2,3)\,. \tag{A17}$$

Here,

$$p_k \equiv \frac{\partial \tau_0}{\partial x_k}\,, \qquad (k=1,2,3) \tag{A18}$$

are components of the slowness vector $\mathbf{p} = [p_1, p_2, p_3]$ at the common midpoint $\mathbf{x}$.

Comparing equation (A16) with the conventional definition of the normal-moveout velocity $V_{\rm nmo}(\mathcal{L})$ along the CMP line $\mathcal{L}$ given by the equation

$$t^2(X,\mathcal{L}) = t_0^2 + \frac{X^2}{V_{\rm nmo}^2(\mathcal{L})}\,, \tag{A19}$$

we conclude that

$$\frac{1}{V_{\rm nmo}^2(\mathcal{L})} = \mathcal{L}\,\mathbf{U}\,\mathcal{L}^{\mathbf{T}}\,. \tag{A20}$$

APPENDIX B: Constructing NMO surface from NMO ellipse

Let us assume that NMO velocity has been measured along three CMP lines with the same common midpoint $\mathbf{x}$. Assume further that these three lines belong to a single plane and allow us to reconstruct the NMO ellipse $\mathbf{W}$ (e.g., Grechka and Tsvankin, 1998a). We select such coordinate frame where the plane specified by our three lines is the $[x_1, x_2]$-plane, so that the NMO surface $\mathbf{U}$ is given by equation (7). Our goal is to express the unknown elements U_{k3} in terms of the measured quantities W_{ij}. This goal can be achieved by differentiating the Christoffel equation (8)

$$F(\mathbf{p},\mathbf{x}) = 0\,. \tag{B1}$$

with respect to x_k. Here, $\mathbf{p} = \mathbf{p}(\mathbf{x})$ is the slowness vector, and F explicitly depends on the CMP coordinate $\mathbf{x}$ because the elastic stiffness coefficients c_{ij} are functions of $\mathbf{x}$ in heterogeneous anisotropic media.

Differentiating equation (B1) with respect to x_1 and x_2 yields

$$\sum_{k=1}^{3} F_{p_k}\,\frac{\partial p_k}{\partial x_j} + F_{x_j} = 0\,, \qquad (j=1,2)\,, \tag{B2}$$

where $F_{p_k} \equiv \partial F/\partial p_k$ and $F_{x_j} \equiv \partial F/\partial x_j$. Assuming the zero-offset traveltime τ_0 to be measured along with NMO ellipse $\mathbf{W}$, we express the partial derivatives of the horizontal slowness components as [see equations (2) and (6)]

$$\frac{\partial p_i}{\partial x_j} = \frac{W_{ij}}{\tau_0}\,, \qquad (i,j=1,2)\,. \tag{B3}$$

Substituting equations (B3) into equations (B2) and solving those equations for $\partial p_3/\partial x_j$, find

$$U_{j3} \equiv \tau_0 \frac{\partial p_3}{\partial x_j} = -\frac{F_{p_1} W_{1j} + F_{p_2} W_{2j} + \tau_0 F_{x_j}}{F_{p_3}}, \qquad (j = 1, 2). \tag{B4}$$

Since $\partial p_j/\partial x_3 = \partial p_3/\partial x_j$ because of the symmetry of the matrix $\mathbf{U}$ [equations (2) and (7)], differentiating the Christoffel equation (B1) with respect to x_3 yields

$$U_{33} \equiv \tau_0 \frac{\partial p_3}{\partial x_3} = -\frac{F_{p_1} U_{13} + F_{p_2} U_{23} + \tau_0 F_{x_3}}{F_{p_3}}. \tag{B5}$$

Next, we fix the CMP location $\mathbf{x}$ and treat the Christoffel equation as an implicit function which relates (locally, at $\mathbf{x}$) the vertical slowness component $p_3 \equiv q$ to the horizontal slowness components p_1 and p_2. Implicit differentiation of the Christoffel equation then gives (Grechka et al., 1999)

$$q_{,j} = -\frac{F_{p_j}}{F_q}, \qquad (j = 1, 2), \tag{B6}$$

where $q_{,j} \equiv \partial q/\partial p_j \equiv \partial p_3/\partial p_j$ and $F_q \equiv \partial F/\partial q \equiv \partial F/\partial p_3$. Using equation (B6), we rewrite equations (B4) and (B5) in the form

$$U_{j3} = q_{,1} W_{1j} + q_{,2} W_{2j} - \tau_0 \frac{F_{x_j}}{F_q}, \qquad (j = 1, 2) \tag{B7}$$

and

$$U_{33} = q_{,1} U_{13} + q_{,2} U_{23} - \tau_0 \frac{F_{x_3}}{F_q}. \tag{B8}$$

Substituting equations (B7) into (B8), we obtain

$$U_{33} = q_{,1}^2 W_{11} + 2 q_{,1} q_{,2} W_{12} + q_{,2}^2 W_{22} - \tau_0 \frac{q_{,1} F_{x_1} + q_{,2} F_{x_2} + F_{x_3}}{F_q}. \tag{B9}$$

APPENDIX C: Dix-type averaging in arbitrarily heterogeneous anisotropic media

Here, we describe the details of building the NMO surfaces in heterogeneous anisotropic media. Let us suppose that we know the NMO surface $\mathbf{U}(\tau_0)$ at traveltime τ_0 of the zero-offset ray and want to construct $\mathbf{U}(\tau_0 + \Delta\tau_0)$ at traveltime $\tau_0 + \Delta\tau_0$, where $\Delta\tau_0$ is the infinitesimal time interval. Our procedure is based on the fact of the existence of the plane $\mathcal{P}(\tau_0)$ orthogonal to the derivative $d\mathbf{p}(\tau_0)/d\tau_0$, where components of the slowness vector $\mathbf{p}(\tau_0)$ are locally preserved (Figure 3). If we make the cross-section of the NMO surface $\mathbf{U}(\tau_0)$ by the plane $\mathcal{P}(\tau_0)$

$$\mathbf{W}^{\mathcal{P}(\tau_0)}(\tau_0) = \mathbf{U}(\tau_0) \bigcap \mathcal{P}(\tau_0),$$

we can apply the Dix-type averaging formula (29) to this cross-section at the infinitesimal ray segment specified by the traveltime $\Delta\tau_0$:

$$\left[\mathbf{W}^{\mathcal{P}(\tau_0)}(\tau_0 + \Delta\tau_0)\right]^{-1} = \frac{\tau_0 \left[\mathbf{W}^{\mathcal{P}(\tau_0)}(\tau_0)\right]^{-1} + \Delta\tau_0 \left[\mathbf{W}^{\mathcal{P}(\tau_0)}\big|_{[\tau_0,\, \tau_0+\Delta\tau_0]}\right]^{-1}}{\tau_0 + \Delta\tau_0}, \tag{C1}$$

where

$$\mathbf{W}^{\mathcal{P}(\tau_0)}\big|_{[\tau_0,\, \tau_0+\Delta\tau_0]} = \mathbf{U}\big|_{[\tau_0,\, \tau_0+\Delta\tau_0]} \bigcap \mathcal{P}(\tau_0)$$

is the cross-section of the local NMO surface $\mathbf{U}\big|_{[\tau_0,\, \tau_0+\Delta\tau_0]}$ at the infinitesimal interval $[\tau_0, \tau_0+\Delta\tau_0]$ by the same plane $\mathcal{P}(\tau_0)$. The NMO surface $\mathbf{U}\big|_{[\tau_0,\, \tau_0+\Delta\tau_0]}$ can be computed using equations (7), (10) and (16).

The plane $\mathcal{P}(\tau_0 + \Delta\tau_0) \perp d\mathbf{p}/d\tau_0\big|_{\tau_0+\Delta\tau_0}$ at traveltime $\tau_0 + \Delta\tau_0$ is generally different from the plane $\mathcal{P}(\tau_0)$ as shown in Figure 3. In order to account for the rotation of the plane $\mathcal{P}$ along the ray, we reconstruct the NMO surface $\mathbf{U}(\tau_0 + \Delta\tau_0)$ from its cross-section $\mathbf{W}^{\mathcal{P}(\tau_0)}(\tau_0 + \Delta\tau_0)$ using equations (D9) and (D12) derived in Appendix D and, then, make another cross-section of $\mathbf{U}(\tau_0 + \Delta\tau_0)$ by the plane $\mathcal{P}(\tau_0 + \Delta\tau_0)$. This gives us the cross-section

$$\mathbf{W}^{\mathcal{P}(\tau_0+\Delta\tau_0)}(\tau_0 + \Delta\tau_0) = \mathbf{U}(\tau_0 + \Delta\tau_0) \bigcap \mathcal{P}(\tau_0 + \Delta\tau_0).$$

Since the slowness components are, again, locally preserved in the plane $\mathcal{P}(\tau_0 + \Delta\tau_0)$, we can continue the cross-section $\mathbf{W}^{\mathcal{P}(\tau_0+\Delta\tau_0)}(\tau_0 + \Delta\tau_0)$ along the next ray segment using equation (C1) written for the time interval $[\tau_0 + \Delta\tau_0,\ \tau_0 + 2\Delta\tau_0]$.

Thus, computing the NMO surfaces in inhomogeneous anisotropic media can be accomplished *simultaneously* with integrating ray equations (30). The continuation of the NMO surfaces involves the following steps:

Step 1. Construct the cross-section $\mathbf{W}^{\mathcal{P}(\tau_0)}(\tau_0)$ [equation (D7)] of the given NMO surface $\mathbf{U}(\tau_0)$ by the plane $\mathcal{P}(\tau_0)$ orthogonal to the vector $d\mathbf{p}/d\tau_0$ specified by the second equation (30).

Step 2. Continue $\mathbf{W}^{\mathcal{P}(\tau_0)}(\tau_0) \rightarrow \mathbf{W}^{\mathcal{P}(\tau_0)}(\tau_0 + \Delta\tau_0)$ using equation (C1).

Step 3. Reconstruct the surface $\mathbf{U}(\tau_0 + \Delta\tau_0)$ [equations (D9) and (D12)] from its cross-section $\mathbf{W}^{\mathcal{P}(\tau_0)}(\tau_0 + \Delta\tau_0)$.

Step 4. Repeat **Step 1** for the surface $\mathbf{U}(\tau_0 + \Delta\tau_0)$.

APPENDIX D: Matrices for continuation the NMO surfaces

In this appendix, we derive the equations to compute the cross-section $\mathbf{W}^{\mathcal{P}}$ of the NMO surface $\mathbf{U}$ by an arbitrary plane $\mathcal{P}$ and to reconstruct the matrix $\mathbf{U}$ back from its cross-section $\mathbf{W}^{\mathcal{P}}$.

Let us denote $\mathbf{z}$ the unit vector in the direction $d\mathbf{p}/d\tau_0$ [see equation (30)] normal to the plane $\mathcal{P}$. The vector $\mathbf{z}$ can be specified by two spherical angles ϕ_1 and ϕ_2:

$$\mathbf{z} = [\sin\phi_1 \cos\phi_2,\ \sin\phi_1 \sin\phi_2,\ \cos\phi_1]\,. \tag{D1}$$

It is straightforward to verify that the unit vectors

$$\mathbf{b}^{(1)} = [\cos\phi_1 \cos\phi_2,\ \cos\phi_1 \sin\phi_2,\ -\sin\phi_1] \tag{D2}$$

and

$$\mathbf{b}^{(2)} = [-\sin\phi_2,\ \cos\phi_2,\ 0] \tag{D3}$$

are both orthogonal to $\mathbf{z}$ and, therefore, lie in the plane $\mathcal{P} \perp \mathbf{z}$. Thus, any vector $\mathbf{b}$ in $\mathcal{P}$ is given by

$$\mathbf{b} = \mathbf{b}^{(1)} \cos\alpha + \mathbf{b}^{(2)} \sin\alpha\,, \tag{D4}$$

where α is the azimuth (within $\mathcal{P}$) with respect to $\mathbf{b}^{(1)}$.

The NMO velocity [equation (1)] within the plane $\mathcal{P}$

$$\frac{1}{V^2_{\rm nmo}(\mathbf{b})} = \mathbf{b}\,\mathbf{U}\,\mathbf{b}^{\mathbf{T}} \tag{D5}$$

can be viewed as the cross-section of the NMO surface $\mathbf{U}$ by the plane $\mathcal{P}$. Substituting equations (D2)–(D4) into (D5) yields

$$\left.\frac{1}{V^2_{\rm nmo}(\alpha)}\right|_{\mathcal{P}} =$$

$$= W^{\mathcal{P}}_{11} \cos^2\alpha + 2\,W^{\mathcal{P}}_{12} \sin\alpha\cos\alpha + W^{\mathcal{P}}_{22} \sin^2\alpha\,, \tag{D6}$$

where

$$W^{\mathcal{P}}_{ij} = \sum_{k,m=1}^{3} B_{km,\,ij}\,U_{km}\,, \qquad (i,j=1,2)\,, \tag{D7}$$

and

$$B_{km,\,ij} = \frac{1}{2}\left(b^{(i)}_k b^{(j)}_m + b^{(j)}_k b^{(i)}_m\right), \qquad (i,j=1,2;\quad k,m=1,2,3)\,. \tag{D8}$$

Equations (D1)–(D3), (D7), and (D8) define the matrix $\mathbf{W}^{\mathcal{P}}$ which describes the cross-section (i.e., the NMO ellipse) of the NMO surface $\mathbf{U}$ by the plane $\mathcal{P}$ with the unit normal $\mathbf{z}$.

Next, we show how to reconstruct the whole NMO surface $\mathbf{U}$ from its cross-section $\mathbf{W}^{\mathcal{P}}$. The reconstruction is based on equations (7) and (10) which we write here in the form

$$\mathbf{U} = \begin{pmatrix} W_{11} & W_{12} & q_{,1}W_{11} + q_{,2}W_{12} + A_1 \\ \bullet & W_{22} & q_{,1}W_{12} + q_{,2}W_{22} + A_2 \\ \bullet & \bullet & q^2_{,1}W_{11} + 2q_{,1}q_{,2}W_{12} + q^2_{,2}W_{22} + A_3 \end{pmatrix}, \tag{D9}$$

where the bullets in the low left-hand corner denote the elements equal to their symmetric ones in the upper right-hand corner, $\mathbf{W}$ is the NMO ellipse in the *horizontal* plane $[x_1, x_2]$,

$$A_i = -\tau_0\,\frac{F_{x_i}}{F_q}\,, \qquad (i=1,2)\,,$$

$$A_3 = -\tau_0\,\frac{q_{,1}F_{x_1} + q_{,2}F_{x_2} + F_{x_3}}{F_q}\,,$$

and the derivatives of F [equation (B1)], which also determine the derivatives of the vertical slowness component $q_{,i}$ and $q_{,ij}$ [equation (B6) and the second equation (16)], are evaluated at point $\mathbf{x}$ of the zero-offset ray specified by the one-way traveltime τ_0.

It is evident from equation (D9) that in order to compute $\mathbf{U}$, we need to know the matrix $\mathbf{W}$ because all the other quantities are obtained by differentiating the Christoffel equation (B1). Substituting equation (D9) into (D7) gives three linear equations which relate elements of the matrices $\mathbf{W}$ and $\mathbf{W}^{\mathcal{P}}$:

$$W^{\mathcal{P}}_{ij} = C_{ij} + \sum_{i',j'=1}^{2} D_{i'j',\,ij}\,W_{i'j'}\,, \qquad (i,j=1,2)\,. \tag{D10}$$

In this equation,

$$C_{ij} = 2A_1B_{13,\,ij} + 2A_2B_{23,\,ij} + A_3B_{33,\,ij}$$

and

$$D_{i'j',\,ij} = B_{i'j',\,ij} + q_{,i'}B_{j'3,\,ij} + q_{,j'}B_{i'3,\,ij} + q_{,i'}q_{,j'}B_{33,\,ij}\,, \qquad (i',j',i,j=1,2)\,.$$

To make more explicit the fact that equations (D10) represent a system of linear equations for unknown elements $W_{i'j'}$, we replace the pairs of indexes $\{ij\}$ and $\{i'j'\}$ by a single index following the pattern: $\{11\} \to 1$, $\{12\} \to 2$, and $\{22\} \to 3$. Then, equations (D10) can be rewritten in more conventional form

$$W^{\mathcal{P}}_k = C_k + \sum_{k'=1}^{3} E_{k'k}\,W_{k'}\,, \qquad (k=1,2,3)\,. \tag{D11}$$

where $E_{k'k}$ are the elements of the 3×3 matrix

$$\mathbf{E} = \begin{pmatrix} D_{11,\,11} & 2\,D_{12,\,11} & D_{22,\,11} \\ D_{11,\,12} & 2\,D_{12,\,12} & D_{22,\,12} \\ D_{11,\,22} & 2\,D_{12,\,22} & D_{22,\,22} \end{pmatrix}.$$

Equations (D11) can be solved in a standard way and the matrix $\mathbf{W}$ is given by

$$\mathbf{W} = \mathbf{E}^{-1}\left(\mathbf{W}^{\mathcal{P}} - \mathbf{C}\right). \tag{D12}$$

Thus, equations (D9) and (D12) along with the Christoffel equation (B1) allow us to reconstruct the NMO surface $\mathbf{U}$ from its cross-section $\mathbf{W}^{\mathcal{P}}$ by the plane $\mathcal{P}$.